



## Research article

# AutoDock and molecular dynamics-based therapeutic potential prediction of flavonoids for primary Sjögren's syndrome

Tianjiao Mao<sup>a</sup>, Bo Chen<sup>a</sup>, Wei Wei<sup>c</sup>, Guiping Chen<sup>a</sup>, Zhuoyuan Liu<sup>a</sup>, Lihong Wu<sup>a</sup>, Xiaomeng Li<sup>b,\*\*\*</sup>, Janak L. Pathak<sup>a,\*</sup>, Jiang Li<sup>a,\*\*</sup>

<sup>a</sup> School and Hospital of Stomatology, Guangdong Engineering Research Center of Oral Restoration and Reconstruction, Guangzhou Medical University, Guangzhou, 510140, China

<sup>b</sup> KingMed School of Laboratory Medicine, Guangzhou Medical University, Guangzhou, 510140, China

<sup>c</sup> Department of Prosthodontics, School and Hospital of Stomatology, Jilin University, Changchun, 130012, China

## ARTICLE INFO

## Keywords:

Primary Sjögren syndrome  
Flavonoids  
ER $\alpha$   
Molecular docking  
Homology modeling  
Molecular dynamics simulations

## ABSTRACT

Primary Sjögren's Syndrome (pSS) is a systemic autoimmune disease that leads to reduced saliva production, primarily affecting women due to estrogen deficiency. The estrogen receptor  $\alpha$  (ER $\alpha$ ) plays a crucial role in mediating the expression of the aquaporin 5 (AQP5) gene through the estrogen response element-dependent signaling pathway, making ER $\alpha$  a key drug target for pSS. Several flavonoids have been reported to have the potential to treat pSS. This study aimed to screen and compare flavonoids binding to ER $\alpha$  using AutoDock, providing a basis for treating pSS with flavonoids. The estrogenic potential of six representative flavonoids was examined in this study. Molecular docking revealed that the binding energy of all six flavonoids to ER $\alpha$  was less than  $-5.6$  kcal/mol. Apigenin, naringenin, and daidzein were the top three flavonoids with even lower binding energies of  $-7.8$ ,  $-8.09$ , and  $-8.59$  kcal/mol, respectively. Similar to the positive control estradiol, apigenin, naringenin, and daidzein showed hydrogen bond interactions with GLU353, GLY521, and HIS524 at the active site. The results of luciferase reporter assays demonstrated that apigenin, naringenin, and daidzein significantly enhanced the transcription of estrogen receptor element (ERE) in the PGL3/AQP5 promoter. Furthermore, molecular dynamics simulations using GROMACS for a time scale of 100 ns revealed relatively stable binding of apigenin-ER $\alpha$ , naringenin-ER $\alpha$ , and daidzein-ER $\alpha$ . Mechanistically, homology modeling indicated that GLU353, GLY521, and HIS524 were the key residues of ER $\alpha$  exerting an estrogenic effect. The therapeutic effect of apigenin on dry mouth in pSS models was further validated. In conclusion, these results indicate the estrogenic and pSS therapeutic potential of apigenin, naringenin, and daidzein.

## 1. Introduction

Primary Sjögren syndrome (pSS) is a chronic autoimmune disease with a worldwide prevalence of approximately 0.1 % [1]. Most

\* Corresponding author.

\*\* Corresponding author.

\*\*\* Corresponding author.

E-mail addresses: [2022990077@gzhmu.edu.cn](mailto:2022990077@gzhmu.edu.cn) (X. Li), [j.pathak@gzhmu.edu.cn](mailto:j.pathak@gzhmu.edu.cn) (J.L. Pathak), [ljiang@gzhmu.edu.cn](mailto:ljiang@gzhmu.edu.cn) (J. Li).

patients have limited symptoms with dry mouth and/or dry eyes, with 30%–40 % of patients having extra glandular manifestations, including interstitial lung disease, cutaneous vasculitis, and lymphomas, thereby increasing their risk of mortality [2,3]. Female subjects are more prone to developing pSS than males with a ratio of 9–19:1 [4–7]. Additionally, the severity of sicca symptoms is also higher in females than males [8]. Overall, studies indicate that gender affects the onset and development of pSS.

There are two peak periods of onset of pSS in women, one during the infant-feeding period around age 30 and more frequently during the postmenopausal period around age 55 [9–11], the phenomenon indicates that estrogen levels affect the onset of pSS. Studies have reported that the serum level of estrogen (E2) correlates with the severity of pSS, while the serum level of progesterone has no significant differences between patients and health controls [12,13]. Moreover, it has been reported that pSS patients with any increased exposure to estrogen such as hormone replacement therapy (HRT) could alleviate the symptoms [14]. E2 exerts its effects primarily by binding to the estrogen receptors (ERs), ERs are expressed in salivary gland epithelium cells (SGECs) and are transcription factors of aquaporin 5 (AQP5), the vital membrane protein of SGECs responsible for water transport [15,16]. Disruption of E2-ER signaling is commonly observed in pSS. Therefore, the activation of E2-ER signaling could be a potential approach to treat pSS.

Currently, clinical treatments for pSS are still severely lacking, it is urgent to screen and develop safe and effective therapeutic drugs. Experts have confirmed that E2 deficiency induces apoptosis and the development of pathogenic autoantigens in SGECs [17]. As for the HRT on pSS, both experimental evidence and clinical case-control studies indicate that HRT exhibits beneficial effects, including fostering anti-inflammatory responses and improving saliva secretion [18–20]. Notably, the benefits and risks of HRT are always vigorously debated, estrogen can have detrimental effects, including increasing the risks of vascular embolism, breast cancer, and stroke [21,22]. Additionally, small-molecule inhibitors targeting autoimmune diseases have been evaluated, they are expensive and their pharmacological effect is minimal [23]. Therefore, the development of targeted drugs with low side effects for pSS treatment should be the focus of future research.

Phytoestrogens elicit beneficial effects without causing side effects related to estrogen [24]. Flavonoids are phytoestrogens that are common in human diets and play essential roles in several biological processes, such as antioxidant effects, anti-inflammatory, and anti-viral activities, which reduce the risk of various diseases [25–28]. There are over 9000 flavonoids have been identified and grouped into six distinct subclasses according to their basic structure, flavones, flavonols, isoflavones, chalcones, anthocyanidins, and aurones [29,30]. Some kinds of flavonoids have been reported to activate ER $\alpha$ , such as apigenin, naringenin, daidzein, chalcone, and pelargonidin [31–34]. However, they belong to different kinds of flavonoids, and their capabilities binding to ER $\alpha$  are unknown [35]. In this study, the representative structures of flavones, flavonols, isoflavones, chalcones, anthocyanidins, and aurones were used to compare the interaction profiles with ER $\alpha$ . Therefore, we could select the better flavonoids to treat pSS.

Computational methods are applied at an early stage to provide valuable insights into understanding the chemical systems virtually and thus complement experimental analysis. *In silico* screening along with *in vitro* and *in vivo* experiments accelerate drug discovery [36]. Molecular docking and Molecular dynamics (MD) can calculate the interaction energies and ligand binding mechanism of protein-ligand complexes [37]. Molecular docking is the most commonly used method for precisely predicting the binding energy and binding sites which helps to evaluate the possibility of interactions and predicts binding modes of ligands to protein based on the knowledge of the 3D structure [38,39]. MD simulation enables the continuous monitoring of conformational dynamics at the atomic level in the binding protein over a period of time [40]. Homogeneous protein modeling utilizes experimentally determined protein structures (templates) to predict the conformation of a protein with a similar amino acid sequence (target) [41]. *In silico*, protein modeling can be employed to predict the 3D protein models and their active sites. The critically active amino acid residues in the structural framework can be analyzed using homogeneous modeling [42]. The relationship between the structure of flavonoids and their estrogenic activity, as well as the binding modes, binding energy, and dynamic stability, is still unknown. These aforementioned tools could be valuable for predicting the interaction between flavonoids and ER $\alpha$ .

This study aimed to validate the interaction between flavonoids and ER $\alpha$  using *in silico* screening as a method to identify potential drugs for treating pSS. We employed molecular docking and MD simulations to determine the binding site of flavonoids on ER $\alpha$ , investigate their dynamics, and identify the crucial amino acid residues involved in ligand binding. Additionally, we conducted a luciferase reporter assay to confirm the activation of ERE following the interaction between flavonoids and ER $\alpha$ . Our findings revealed that flavones, flavanones, and isoflavones exhibit strong and stable binding energies with ER $\alpha$ , leading to ERE activation.

## 2. Materials and methods

### 2.1. Materials

E2, apigenin, naringenin, daidzein, chalcone, pelargonidin, and aureusidin (purity, HPLC $\geq$ 98 %) were purchased from Baoji Herbest Bio-Tech (Xian, China). EZ-Trans was purchased from LIFE iLAB BIO (Shanghai, China). Luc-Pair™ Duo-Luciferase Assay Kit was purchased from GeneCopoeia™ (Rockville, MD, USA).

### 2.2. Preparation of three-dimensional (3D) structures of the ligands and receptor molecules for docking

For protein receptor preparation, the 3D structure of ER $\alpha$  (PDB ID: 3ERD) was downloaded from the PDB ([www.rcsb.org/pdb](http://www.rcsb.org/pdb)), next, water and other binding ligands were removed, the modified structure was saved in PDB format using PyMOL software. Furthermore, the polar hydrogens and Kollman charges were added to the processed PDB file, and the energy was minimized using Python Molecular Viewer. Finally, the AutoDock protein format (PDBQT) file was generated and used for subsequent computational docking studies.

For ligands preparation, the 3D chemical structures of the positive control E2 (PubChem CID: 5757), negative control octahydroindolizine (PubChem CID: 26136), and six representative flavonoids, including apigenin (flavones; PubChem CID: 5280443), naringenin (flavanones; PubChem CID: 932), daidzein (isoflavones; PubChem CID: 5280961), chalcone (chalcones; PubChem CID: 637760), pelargonidin (anthocyanidins; PubChem CID: 440832), and aureusidin (aurones; PubChem CID: 5281220) were retrieved from PubChem (<https://pubchem.ncbi.nlm.nih.gov>) [43]. Next, the downloaded SDF format files were converted to PDB format files using PyMOL software. Then, the number of torsions was set, the neutral position (pH = 7) was charged, and the energies were minimized in the Python Molecular viewer. Finally, PDBQT files were saved and used for further studies.

### 2.3. Molecular docking and MD

AutoDock 4.2 was used to perform the docking of ligands to the ER $\alpha$  following the protocol reported previously [44]. The PDBQT formats of ligands and ER $\alpha$  were opened, and the grid box was set to cover the ER $\alpha$  surface to facilitate the unrestricted movement of the ligands. Importantly, all the center grid boxes were set to be the same for different ligands in this study, and the X, Y, and Z centers were always the same: the X center was 19.613, the Y center was -18.981, and the Z center was -5.888. The Autogrid program was run after these settings were made. After the grid program ran, the macromolecule was set as a rigid filename and the Lamarck genetic algorithm (LGA) was set as the docking algorithm, then the AutoDock program was run. 100 poses were generated and poses with the best energy score were selected and analyzed. Finally, figures were generated using Pymol software.

Gromacs2022.3 software was used for MD simulations of the top three flavonoids and E2 with the protein 3ERD. AmberTools22 was used to add GAFF force field to ligands, while Gaussian 16W was used to hydrogenate ligands and calculate RESP potential. Potential data will be added to the topology file of the MD system. The simulation conditions were carried out at a static temperature of 300K and atmospheric pressure (1 Bar). Amber99sb-ildn was used as a force field, water molecules were used as a solvent (Tip3p water model), and the total charge of the simulation system was neutralized by adding an appropriate number of Na<sup>+</sup> ions. The simulation system adopts the steepest descent method to minimize the energy, and then carries out the isothermal isovolumic ensemble (NVT) equilibrium and isothermal isobaric ensemble (NPT) equilibrium for 100000 steps, respectively, with the coupling constant of 0.1 ps and the duration of 100 ps. Finally, the free molecular dynamics simulation was performed. The process consisted of 5000000 steps, the step length was 2 fs, and the total duration was 100 ns. After the simulation was completed, the built-in tool of the software was used to analyze the root-mean-square variance (RMSD), root-mean-square fluctuation (RMSF), the number of hydrogen bonds, and solvent-accessible surface area (SASA).

### 2.4. Cell culture and luciferase reporter assay

The HEK293T cells were seeded and cultured in DMEM containing 10 % fetal bovine serum and incubated at 37 °C in a humidified incubator with 5 % CO<sub>2</sub>, when passaged, the cells were plated into 48-well plates at a density of  $1 \times 10^5$  cells/well, cells in each well were transfected with 100 ng ERE-TATA-luc plasmid and 25 ng pREP7 plasmid for 48 h after 12h, the cells were stimulated with apigenin (1  $\mu$ M), naringenin (1  $\mu$ M), daidzein (1  $\mu$ M), chalcone (1  $\mu$ M), pelargonidin (1  $\mu$ M), aureusidin (1  $\mu$ M), or E2 (0.1  $\mu$ M) for 24 h. Cell lysates were collected to measure the firefly and renilla luciferase activities. The corresponding absorbance was detected using the microplate reader according to the manufacturer's protocol. The ratio of firefly luciferase activity to renilla luciferase activity was calculated as relative luciferase activity.

### 2.5. Homology modeling

Homology modeling simulation was performed using SWISS-MODEL (<https://swissmodel.expasy.org/interactive>) and Molecular AutoDock was done as previously described [45]. In comparative modeling, a 3D protein model of the target sequence was generated using the amino acid sequence of the target protein provided in FASTA format, and the data provided served as a query to search for evolutionary-related protein structures against the SWISS-MODEL template library SMTL. Subsequently, templates were ranked based on the expected quality of the resulting models. Finally, the top-ranked template was selected based on the Global Model Quality Estimate (GMQE) and Quaternary Structure Quality Estimate (QSQE) scores for further molecular docking analysis using AutoDock, and the binding energies and binding sites were estimated.

### 2.6. Animal experiments

Female Institute of Cancer Research (ICR) mice (6–8 weeks old, 20–22 g) were purchased from the Hua Fukang Biotechnology Co., Ltd. (Beijing, China). All mice were maintained in a specific pathogen-free animal facility and kept under conventional conditions with free access to food and water. Animals were environmentally adapted for 7 days before starting experiments. All animal studies were approved by the Animal Care and Use Committee at the Institute of Laboratory, Guangzhou Medical University (Protocol number: G2023-147).

### 2.7. Water intake and saliva flow rate assessment

The water intake index for each group was calculated as water intake (mL) divided by body weight (g), and changes within each group were documented. The saliva flow rate was measured once a month after an overnight fast as described previously. Briefly, mice

were anesthetized and then injected with pilocarpine hydrochloride (0.1 mg/kg i.p.). Saliva was collected into pre-weighed tubes using glass capillaries for 10 min, and the tubes were re-weighed. The saliva flow rate was calculated as the increase in weight (mg) divided by body weight (g) divided by 10 min.

## 2.8. Immunohistochemistry

The submandibular gland tissue sections were blocked for 30 min and then incubated with g anti-aquaporin 5 (AQP5, Abcam, ab305304) at a dilution of 1:100 at 4 °C for 16 h. The next day, slices were washed with PBS, followed by the addition of the secondary antibody for 1 h at room temperature, and after the diaminobenzidine (DAB) solution was incubated for 1 min and counterstained with hematoxylin. Quantification of representative images at 100X magnification was carried out by an independent observer.

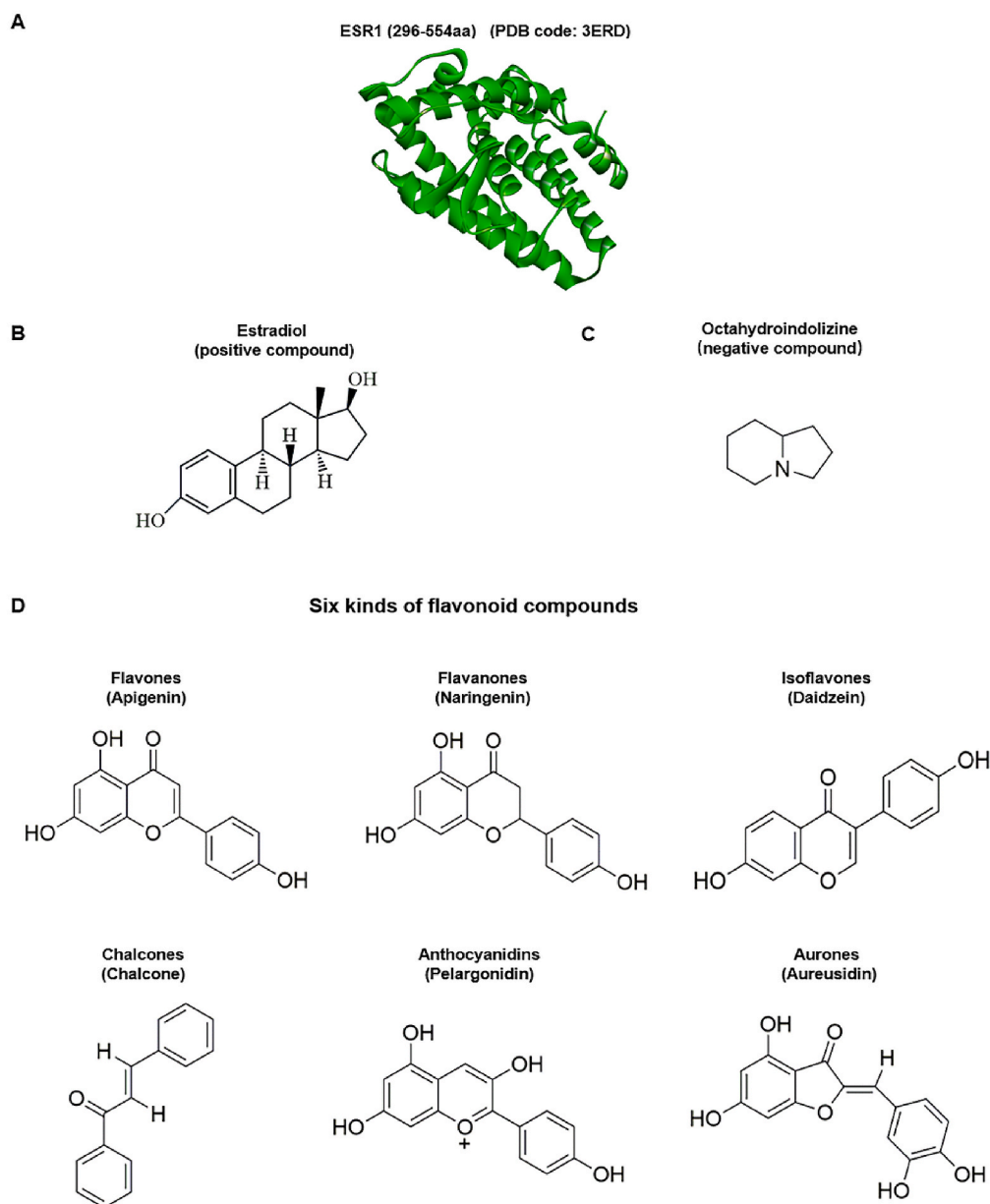


**Fig. 1.** Structure of ER $\alpha$  (ESR1) and ligands. (A) the structure of ER $\alpha$ , (B) the 2D structure of positive control estradiol (C) the 2D structure of negative control octahydroindolizine, and (D) the representative 2D structure of six subclasses of flavonoids.

## 2.9. Statistical analysis

All data are expressed as mean  $\pm$  standard deviation (SD) of three independent experiments. Statistical significance from the control group was evaluated using one-way analysis of variance (ANOVA) using Prism software (GraphPad Software Inc, La Jolla, CA, USA).

## 3. Results

### 3.1. Structure of ligands and ER $\alpha$

The protein ER $\alpha$  (PDB: 3ERD) was downloaded from the Protein Data Bank (PDB [46]) and all the hetero atoms, ligands, and water

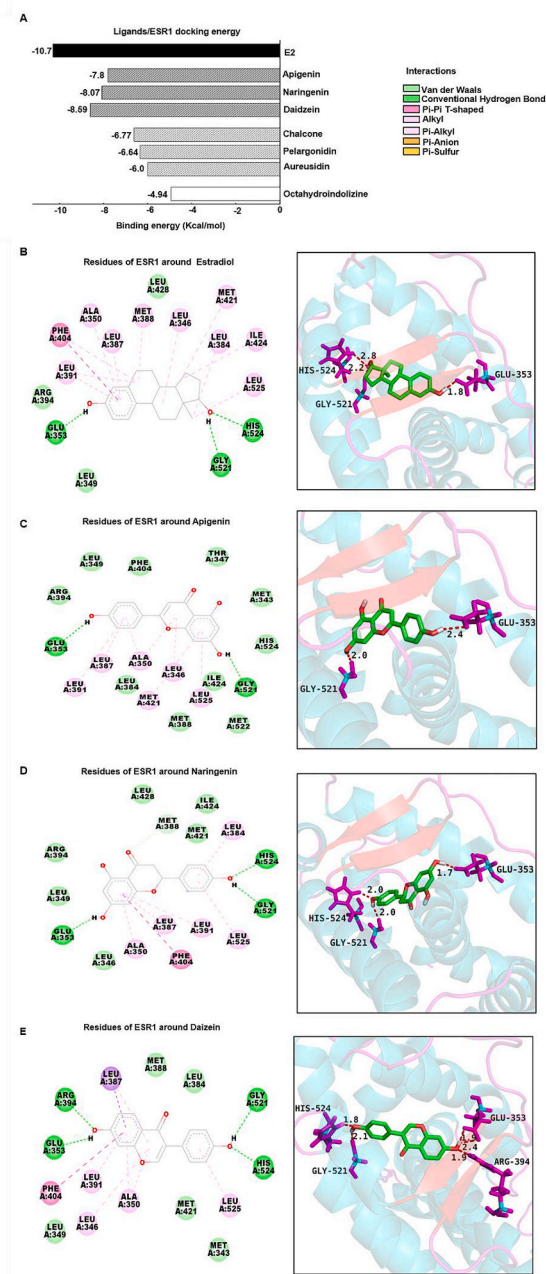


**Fig. 2.** Molecular docking results of ER $\alpha$  with ligands. (A) Comparison of ligands-ER $\alpha$  binding energies. Interaction profile of E2-ER $\alpha$  (B), apigenin-ER $\alpha$  (C), naringenin-ER $\alpha$  (D), and daidzein-ER $\alpha$  (E).

were removed (Fig. 1A), E2 (Fig. 1B) was selected as a positive control, while octahydroindolizine (Fig. 1C) belonging to alkaloids [47] was set as a negative control, and six representative flavonoid compounds (Fig. 1D) were analyzed in this study.

### 3.2. Analysis of binding energies and binding sites of flavonoids with ER $\alpha$

Molecular docking was performed using AutoDock software to analyze the binding energies of flavonoids with ER $\alpha$  [48], lower binding energy indicates a higher binding ability, and the binding energy  $< -7.0$  kcal/mol indicates a very strong binding affinity between the ligand and protein [49]. The results indicated a strong binding affinity between E2 and ER $\alpha$ , with the lowest binding energy of  $-10.29$  kcal/mol, while octahydroindolizine and ER $\alpha$  exhibited the weakest binding affinity, with the highest binding energy of  $-4.94$  kcal/mol. Among the six flavonoids, apigenin, naringenin, and daidzein demonstrated excellent binding affinities with ER $\alpha$ , having binding energies of  $-7.8$ ,  $-8.07$ , and  $-8.59$  kcal/mol, which are all lower than  $-7.0$  kcal/mol. In contrast, chalcone, pelargonidin, and aureusidin displayed weaker binding affinities with ER $\alpha$ , with higher binding energies of  $-6.61$ ,  $-6.34$ , and  $-6.00$  kcal/mol (Fig. 2A). Additionally, we analyzed the intermolecular interactions of the ligands-ER $\alpha$  and found excellent binding affinities. Our results indicated that among E2, apigenin, naringenin, and daidzein with ER $\alpha$ , E2 exhibited promising hydrophobic and hydrophilic interactions with ER $\alpha$ . The important amino acids of the active sites participated in hydrophobic interactions, including conventional hydrogen bonds, van der Waals interactions, pi-pi T-shaped, alkyl, pi-alkyl pi-anion, and pi-sulfur interactions, the crucial molecular interactions involved amino acid residues LEU428, LEU346, MET421, LEU384, ILE424, LEU525, HIS524, GLY521, MET388, LEU387, ALA350, PHE404, LEU391, ARG394, GLU353, and LEU349. Additionally, there are three conventional hydrogen bonds with GLU353, GLY521, and HIS524 at bond distances of 1.8, 2.2, and 2.8 Å (Fig. 2B). Similarly, apigenin formed two H-bonds with GLU353 and GLY521 at 2.4 and 2.0 Å (Fig. 2C). Naringenin formed three H-bonds with GLU353, GLY521, and HIS524 at 1.7, 2.0, and 2.0 Å (Fig. 2D). Daidzein formed five H-bonds, among these, two H-bonds were formed with GLU353 at 1.9 and 2.4 Å, and the other three H-bonds were formed with ARG394, GLY521, and HIS524 at 1.9, 1.8, and 2.1 Å (Fig. 2E). All H-bonds contribute toward the stability of conformations.

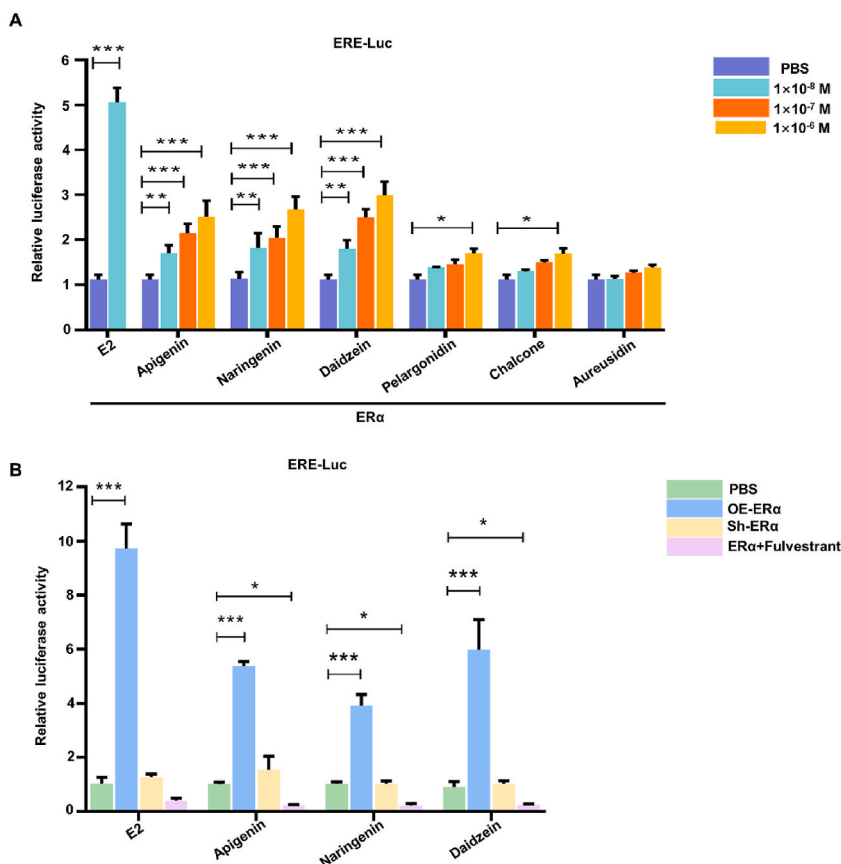


**Fig. 3.** Flavonoids upregulate ERE transcription. (A) Relative luciferase activity shows the EREp activation induced by E2 and flavonoids in salivary gland epithelium cells. (B) Relative luciferase activity shows the EREp activation patterns upon E2, apigenin, naringenin, and daidzein treatment in OE-ER $\alpha$ , sh-ER $\alpha$ , and Fulvestrant-treated SGEcs. Data are presented as the mean  $\pm$  SD,  $n = 3$ . Significant difference between the groups, \* $p < 0.05$ , \*\* $p < 0.01$ , and \*\*\* $p < 0.001$ . sh, knockdown; OE, overexpression.

### 3.3. Dual-luciferase reporter assay

We performed dual-luciferase reporter assays to screen the flavonoids activating the transcription of estrogen-response element (ERE) in the PGL3/AQP5 promoter. The transfected cells were induced using PBS, E2 at  $10^{-8}$  M concentrations, or flavonoids (apigenin, naringenin, daidzein, chalcone, pelargonidin, and aureusidin) at  $10^{-8}$  M,  $10^{-7}$  M, and  $10^{-6}$  M concentrations. The results showed that E2 enhanced transcriptional activity of ERE by approximately 5-fold. The ERE transcriptional activity activation ability of flavonoids increased with higher concentrations and elicited the most potent activation ability at a concentration of  $10^{-6}$  M concentration. Apigenin, naringenin, and daidzein at  $10^{-6}$  M concentration induced ERE transcription by 2-3-fold, with daidzein inducing the highest ERE transcriptional activity ( $\sim$ 3-fold). Chalcone and pelargonidin at  $10^{-6}$  M concentration induced ERE transcriptional activity by 1.5-fold, and aureusidin at  $10^{-6}$  M concentration did not have an impact on ERE transcriptional activity (Fig. 3A). These results further indicate that apigenin (flavones), naringenin (flavanones), and daidzein (isoflavones) have the potential to activate ERE transcriptional activity in the AQP5 promoter, of which, the daidzein has the most significant effect. Anthocyanidins, chalcones, and aurones are less effective in activating ERE transcription. To further detect whether the flavonoids activate the transcription level of the ERE promoter by binding to ER $\alpha$ , cells were pre-treated with the sh-ER $\alpha$  plasmid, OE-ER $\alpha$  plasmid, or fulvestrant before E2 at  $10^{-8}$  M concentration, apigenin, naringenin, and daidzein at  $10^{-6}$  M concentration were added to cells. The results showed that E2, apigenin, naringenin, and daidzein significantly induced ERE transcription after transfection with OE-ER $\alpha$  plasmid. However, when cells were pretreated with fulvestrant or sh-ER $\alpha$  plasmid, the transcription of ERE in the AQP5 promoter was down (Fig. 3B). These results indicate that apigenin (flavones), naringenin (flavanones), and daidzein (isoflavones) can activate the transcriptional activity of ERE in the AQP5 promoter and have the potential treatment on pSS via ER $\alpha$ /AQP5 signaling in salivary gland epithelium cells.

### 3.4. MD simulation

To further estimate the stability of intermolecular interactions produced between ER $\alpha$  and E2, apigenin, naringenin, or daidzein, MD simulation during 100 ns was performed on the complexes. the MD simulations were Performed at three replicas to get a reliable analysis.

#### 3.4.1. Analysis of RMSD and RMSF

To determine the stability of each system during the simulations, RMSD was calculated. The stability of apigenin, naringenin, and daidzein, when bound with ER $\alpha$ , was analyzed and compared with E2. The results showed the RMSD track of E2 fluctuated between 0.0 and 0.05 nm during MD simulation, and the average RMSD value was 0.25 nm, ER $\alpha$ -E2 stabilized with an RMSD value of  $0.23 \pm 0.05$  nm during 100 ns of MD simulation (Fig. 4A and Fig. S1A). Analysis of apigenin bound with ER $\alpha$  showed a stabilization around 0.25  $\pm$  0.05 nm after 16 ns which was maintained up to 100 ns (Fig. 4B and Fig. S1B), Similarly, the results obtained for naringenin were

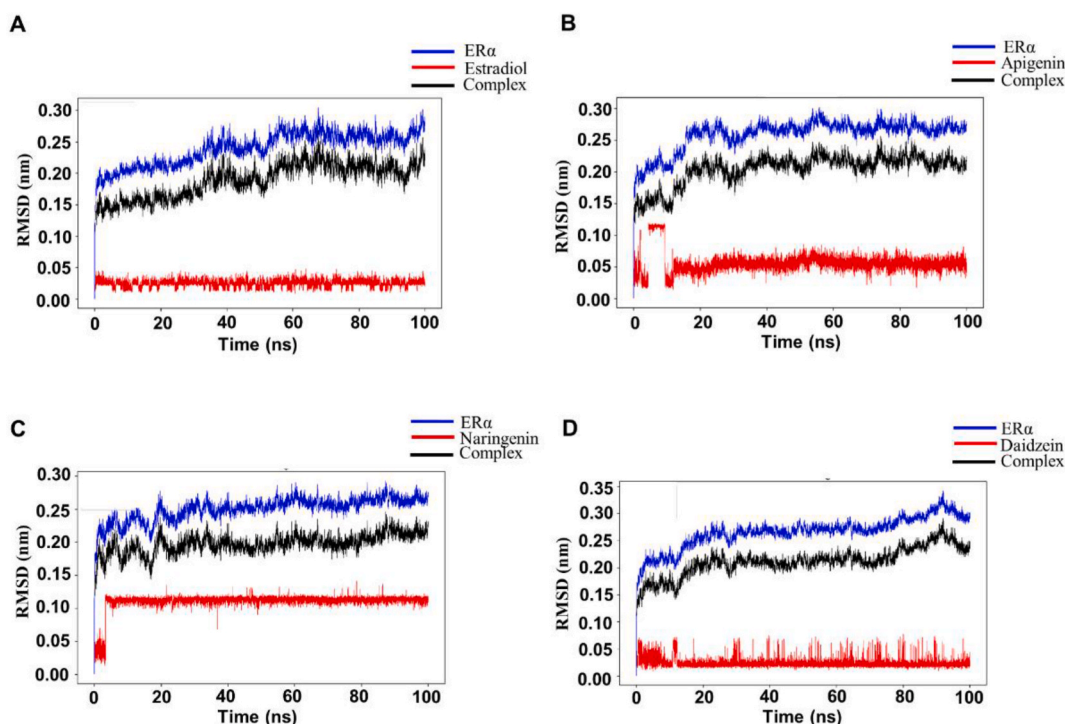


Fig. 4. Root mean square deviation of ER $\alpha$  in the presence of (A) estradiol, (B) apigenin, (C) naringenin, and (D) daidzein at 0 and 100ns.

showed a stabilization around  $0.22 \pm 0.05$  nm after 5 ns which was maintained up to 100 ns (Fig. 4C and Fig. S1C), and ER $\alpha$ -daidzein stabilized with an RMSD value of  $0.25 \pm 0.05$  nm during 100 ns of MD simulation (Fig. 4D and Fig. S1D). These results indicate the stability of apigenin-ER $\alpha$ , naringenin-ER $\alpha$ , and daidzein-ER $\alpha$  during MD simulations.

Analysis of RMSF of individual residues in a protein was performed to understand its flexibility. The results showed the RMSF of chains A and B from the dimer showed similar peaks, and in these studied systems, the RMSF changes were similar, residues with significant changes in RMSF are mainly located at the region of 330–345, 455–475 with RMSF ranging between 0.4 nm and 0.6 nm respectively (Fig. 5A–D and Figs. S2A–D), suggesting stable apigenin-ER $\alpha$ , naringenin-ER $\alpha$ , and daidzein-ER $\alpha$  complexes.

### 3.4.2. Hydrogen bond analysis and SASA

Intermolecular hydrogen bond interactions between the ligand and protein restrict the internal motion of the protein and increase its stability, and the stable number of hydrogen bonds was conducive to the formation of a stable composite system [50], the results showed apigenin, naringenin, and daidzein have stable hydrogen bonds (Fig. 6 A–D and Figure S3 A–D). The SASA is the biological surface area accessible to the solvent, the surface trajectory of the target molecule was obtained by rolling the spherical probe [51]. The SASA area showed apigenin-ER $\alpha$ , naringenin-ER $\alpha$ , and daidzein-ER $\alpha$  ranged at 210–230 nm<sup>2</sup> similar to E2-ER $\alpha$  (Fig. 7 A–D and Figure S4 A–D).

### 3.5. Homology modeling analysis

In this study, the main common active amino acid residues of ER $\alpha$  with apigenin, naringenin, and daidzein were similar between ER $\alpha$  and E2, including GLU353, GLY521, and HIS524 (Table 1). These active amino acid residues have been demonstrated to be specific binding sites in previous studies [52,53].

Homology modeling analysis was performed to verify the importance of GLU353, GLY521, and HIS524. When the GLU353 amino residue was mutated to E353R, the binding site of apigenin-E353R was not in the active binding pocket. Simultaneously, the binding energies of estradiol and flavonoids with E353R were decreased ( $>-6.0$  kcal/mol, Fig. 8A). Similarly, when the amino residues GLY521 and HIS524 mutated to G521R and H524 M, respectively, the binding sites were altered, leading to a significant increase in binding energy and a reduction in binding force (Fig. 8B and C). These results highlight the importance of GLU353, GLY521, and HIS524 of ER $\alpha$  with flavonoids in determining the binding mode and binding energy.

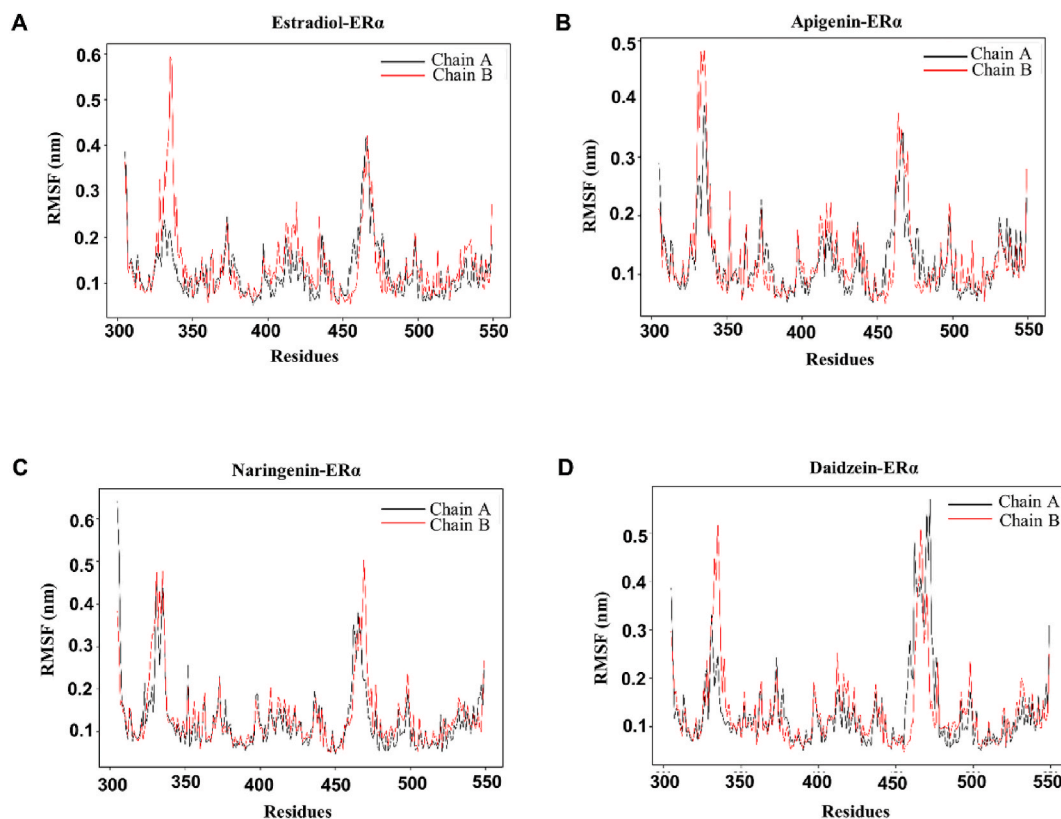


**Fig. 5.** The root mean square fluctuation (RMSF) of ER $\alpha$  in the presence of (A) estradiol, (B) apigenin, (C) naringenin, and (D) daidzein at 0 and 100 ns.



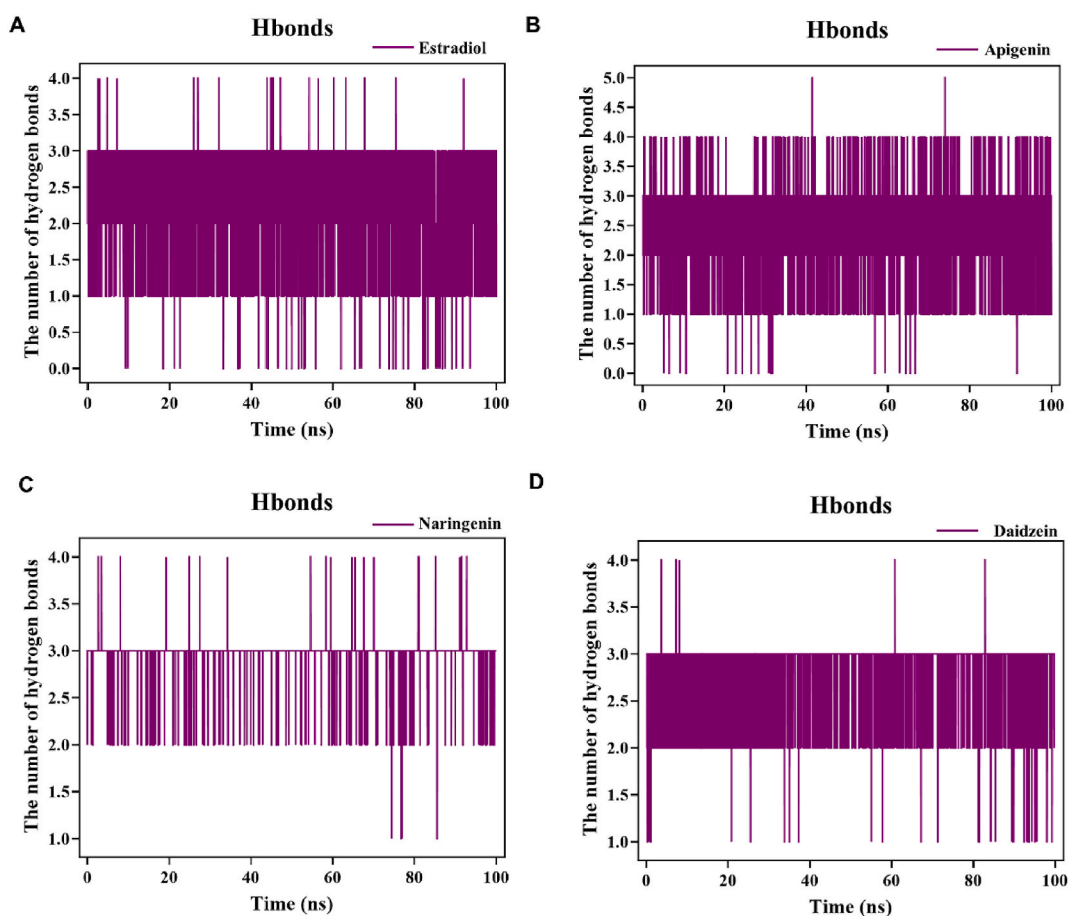


**Fig. 6.** Intermolecular hydrogen bonding pattern in the complex during the simulation time (ns) (A) estradiol-ER $\alpha$ , (B) apigenin-ER $\alpha$ , (C) naringenin-ER $\alpha$ , and (D) daidzein-ER $\alpha$  binding.

### 3.6. Apigenin treatment alleviated xerostomia and revitalized salivary gland function in ovariectomy (OVX) model mice

We have found there is strong binding energy between apigenin and ER $\alpha$ , so, we hypothesized that apigenin has the potential to treat pSS. To verify its effect, The ICR mice were divided randomly into three groups, including sham operation, OVX/control, and OVX/apigenin with six mice in each group. The saliva flow rates were almost the same with no statistical difference before ovariectomy. The saliva secretion in the sham operation group did not change significantly at various stages, 4 weeks after OVX, the saliva secretion in both the control and apigenin groups decreased sharply, while at the 8 weeks and 12 weeks, the saliva secretion of the apigenin group increased gradually and almost reached the level of the sham operation group at 12 weeks. The saliva secretion of the OVX/model group continuously decreased at 8 weeks and 12 weeks (Fig. 9A).

Meanwhile, we measured the water intake before ovariectomy and after 4, 8, and 12 weeks of treatment. The results showed the water intakes were almost the same with no statistical difference before ovariectomy. The water intake in the sham operation group did not change significantly at various stages, 4 weeks after OVX, the water intake in both the control and apigenin groups increased, while at the 8 weeks and 12 weeks, the water intake of the apigenin group decreased gradually and almost reached the level of the sham operation group at 12 weeks. The water intake of the OVX/model group continuously increased at 8 weeks and 12 weeks (Fig. 9B). The results mean that apigenin relieves the dry mouse symptoms in OVX mice.

Next, we did immunohistochemistry (IHC) of AQP5 in the submandibular gland. As the results showed, in the sham operation group, AQP5 was distributed at the membrane of acinar cells, in the OVX group, AQP5 expression was down, While AQP5 expression in the OVX/apigenin group was increased approaching the expression of the sham operation group at the membrane of acinar cells (Fig. 9C). These results indicate that apigenin can upregulate the expression of AQP5 in the submandibular glands in OVX mice.

## 4. Discussions

ER $\alpha$  is expressed in normal salivary gland epithelium and mediates immunomodulatory effects [54,55]. We consider ER $\alpha$  may be an important drug target to treat pSS. Previous studies have analyzed the binding potential of different single flavonoids with ER $\alpha$ .

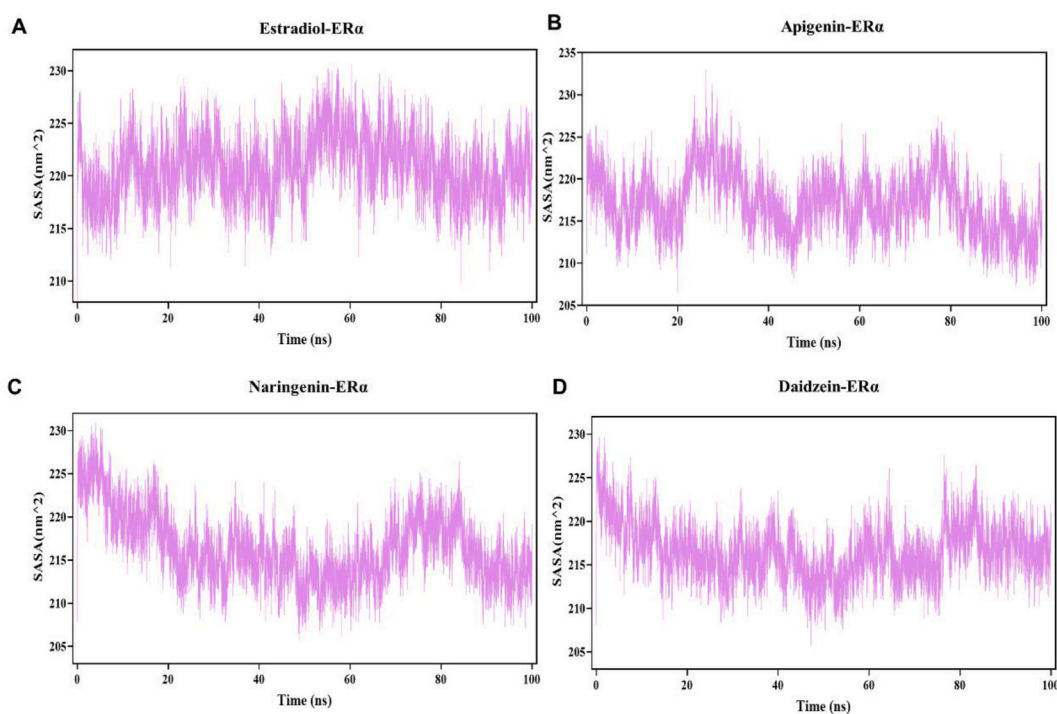


Fig. 7. Analysis of SASA of (A) estradiol-ER $\alpha$ , (B) apigenin-ER $\alpha$ , (C) naringenin-ER $\alpha$ , and (D) daidzein-ER $\alpha$  binding.

Table 1

Docking sites and binding energy of the docking calculation of ER $\alpha$  with flavonoids.

	Name of compound	Pub chem CID	Hydrogen bond	Binding energy (kcal/mol)
Natural hormone	17-beta-estradiol	5757	GLU353, GLY521, HIS524	-10.29
Flavonoids	Apigenin	5280443	GLU353, GLY521	-7.8
	Naringenin	439246	GLU353, GLY521, HIS524	-8.07
	Daidzein	5281708	GLU353, ARG394, GLY521, HIS 524	-8.59
	Chalcone	637760	/	-6.61

However, which flavonoid structure has better binding potential with ER $\alpha$  exerting an estrogenic effect at the cellular level remains unclear. In this study, we compared the binding potential of 6 different flavonoid structures apigenin, naringenin, daidzein, chalcone, pelargonidin, and aureusidin with ER $\alpha$  and the estrogenic effect. We found that among these tested structures apigenin, naringenin, and daidzein showed better binding potential with ER $\alpha$ , suggesting flavones, flavanones, and isoflavones as potential therapeutic agents for pSS treatment.

The vital amino acids, including GLU353, ARG394, GLY 521, and HIS 524 have been reported to be present in the agonists of ER $\alpha$  [56], providing pharmacological therapies for Alzheimer's disease and breast cancer [57,58]. Based on our research, apigenin, naringenin, and daidzein have similar hydrogen bonds with E2-ER $\alpha$ , including ARG394, GLU353, GLY 521, and HIS 524. These results suggest that apigenin, naringenin, and daidzein can act similarly to E2, as the potential natural phytoestrogens to treat pSS. Structural modeling of the flavonoids-ER $\alpha$  complexes may reveal unknown driving factors for pSS treatment, and it provides the basis to modify the drug structures to exert better effects, thereby contributing to the development of better and safer therapy [59]. In the present study, based on AutoDock and MD analysis, we concluded that ligands binding to GLU353, GLY 521, and HIS 524 of ER $\alpha$  were the key to exerting estrogenic effects by apigenin, naringenin, and daidzein.

Aquaporin 5 (AQP5), mainly expressed in salivary gland epithelium cells, plays an important role in salivary secretion, AQP5 knockout mice are reported to have a decrease in saliva flow [60]. Studies have shown that E2 could bind to the ERE on the promoter region of the AQP5 to activate AQP5 expression [61]. Previous studies from others and our research group revealed that E2/ER $\alpha$  signaling regulates AQP5 expression *via* ERE in salivary gland epithelial cells [16,62]. Among the six representative flavonoids, apigenin, naringenin, and daidzein were found to activate the transcriptional activity of ERE in the AQP5 promoter significantly, and daidzein induced the highest ERE transcriptional activity. Then we randomly selected apigenin for *in vivo* experiments and found in the OVX model, that apigenin upregulated the expression of AQP5 significantly. These results further confirmed the estrogenic activity of these flavonoids in SGECs.

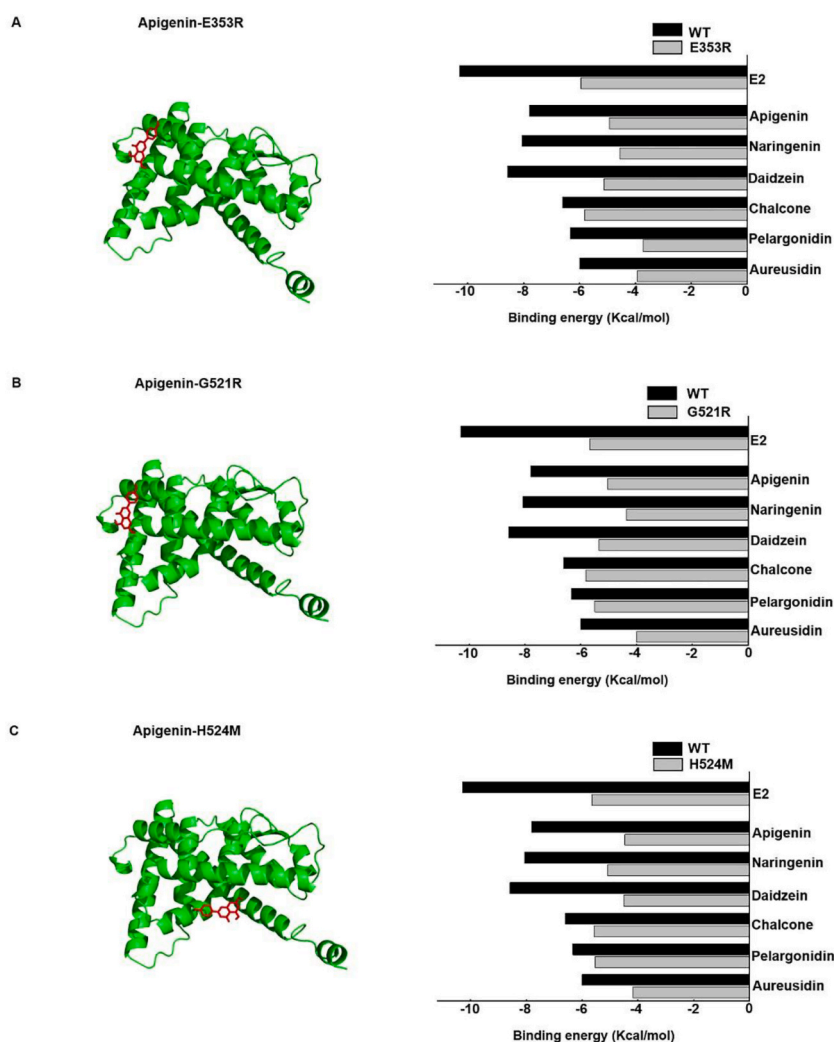


**Fig. 8.** Homology modeling of ER $\alpha$  with flavonoids. (A) the apigenin-E353R complex (left panel) and ligand/E353R binding energy. (B) the apigenin-H521R complex (left panel) and ligand/H521R binding energy. (C) the apigenin-H524 M complex (left panel) and ligand/H524 M binding energy.

## 5. Conclusions

In the present study, the interaction between the human ER $\alpha$  and 6 different flavonoids was analyzed using computational tools Auto Dock 4.2 and GROMACS to probe their estrogenic potential. Docking results showed and MD simulations for 100 ns showed apigenin, naringenin, and daidzein exhibited similar interaction pattern to the positive control E2, Homology modeling showed the acid amino acids GLU353, GLY521, and HIS524 contributed significantly to the molecular mechanism for stabilizing the ligands-ER $\alpha$  complexes and triggering the estrogenic activity of these compounds. Furthermore, we found apigenin, naringenin, and daidzein could activate the transcriptional activity of ERE in the AQP5 promoter, and apigenin could upregulate AQP5 expression and alleviate xerostomia in OVX mice *in vivo*. In conclusion, our results revealed the possible therapeutic potential of apigenin, naringenin, and daidzein as ER $\alpha$  agonists in the treatment of pSS. Further *in vivo* and *in vitro* studies to evaluate the effects of these flavonoids in revitalizing the salivary gland function in pSS are necessary to validate our results.

## Data availability statement

The data that support the findings of this study are available upon reasonable request from the corresponding author. Researchers interested in accessing the data can contact Jiang Li via email at [ljiang@gzhmu.edu.cn](mailto:ljiang@gzhmu.edu.cn).

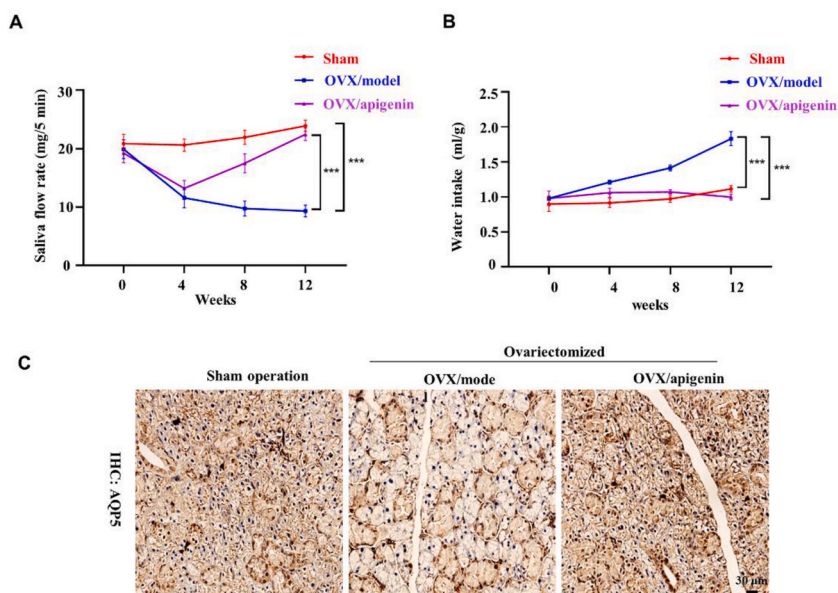


**Fig. 9.** Apigenin ameliorates salivary gland secretion disorders in OVX mice. (A) salivary flow rate before ovariectomy and after 4, 8, and 12 weeks of treatments. (B) water intake before ovariectomy and after 4, 8, and 12 weeks of treatments. (C) immunohistochemistry of AQP5 in submandibular glands. Data are presented as the mean  $\pm$  SD,  $n = 6$ . Significant difference between the groups, \* $p < 0.05$ , \*\* $p < 0.01$ , and \*\*\* $p < 0.001$ .

## Funding

This study was supported by the National Key Research and Development Program of China (2021YFE0108000), and the National Natural Science Foundation of China (82301107).

## Disclosure statement

The authors report there are no competing interests to declare in this paper.

## ORCID iD authorship contribution statement

**Tianjiao Mao:** Writing – original draft, Visualization, Software, Methodology, Formal analysis, Data curation. **Bo Chen:** Writing – original draft, Methodology, Data curation. **Wei Wei:** Project administration, Methodology, Funding acquisition. **Guiping Chen:** Writing – review & editing, Validation, Methodology. **Zhuoyuan Liu:** Visualization, Methodology. **Lihong Wu:** Writing – review & editing, Supervision, Methodology, Investigation. **Xiaomeng Li:** Writing – review & editing, Validation, Supervision, Project administration, Investigation, Conceptualization. **Janak L. Pathak:** Writing – review & editing, Supervision, Data curation, Conceptualization. **Jiang Li:** Supervision, Resources, Project administration, Investigation, Funding acquisition, Formal analysis, Data curation, Conceptualization.

## Declaration of competing interest

The authors declare the following financial interests/personal relationships which may be considered as potential competing interests: Li Jiang reports financial support was provided by the National Key Research and Development Program of China. Wei Wei reports financial support was provided by the National Natural Science Foundation of China. If there are other authors, they declare that they have no known competing financial interests or personal relationships that could have appeared to influence the work reported in this paper.

## Appendix A. Supplementary data

Supplementary data to this article can be found online at <https://doi.org/10.1016/j.heliyon.2024.e33860>.

## References

- [1] M. Ramos-Casals, P. Brito-Zerón, A. Sisó-Almirall, X. Bosch, Primary Sjögren syndrome, *Bmj* 344 (2012) e3821.
- [2] A. Omma, D. Tecer, O. Kucuk Sahin, S.C. Sandikci, F. Yildiz, S. Erten, Do the European League against Rheumatism (EULAR) Sjögren's syndrome outcome measures correlate with impaired quality of life, fatigue, anxiety and depression in primary Sjögren's syndrome? *Arch. Med. Sci.* 14 (4) (2018) 830–837.
- [3] M. Beydon, S. McCoy, Y. Nguyen, T. Sumida, X. Mariette, R. Seror, Epidemiology of sjögren syndrome, *Nat. Rev. Rheumatol.* 20 (3) (2024) 158–169.
- [4] P.C. Hsu, J.W. Chiu, Y.C. Yang, M.J. Jeng, Carpal tunnel syndrome in autoimmune rheumatic diseases and inflammatory bowel diseases: retrospective population cohort study, *Am. J. Phys. Med. Rehabil.* 100 (8) (2021) 760–765.
- [5] M. Ramos-Casals, P. Brito-Zerón, B. Kostov, A. Sisó-Almirall, X. Bosch, D. Buss, A. Trilla, J.H. Stone, M.A. Khamashta, Y. Shoenfeld, Google-driven search for big data in autoimmune geoepidemiology: analysis of 394,827 patients with systemic autoimmune diseases, *Autoimmun. Rev.* 14 (8) (2015) 670–679.
- [6] G.E. Thorlacius, A. Björk, M. Wahren-Herlenius, Genetics and epigenetics of primary Sjögren syndrome: implications for future therapies, *Nat. Rev. Rheumatol.* 19 (5) (2023) 288–306.
- [7] A.L. Stefanski, C. Tomiak, U. Pleyer, T. Dietrich, G.R. Burmester, T. Dörner, The diagnosis and treatment of Sjögren's syndrome, *Dtsch Arztebl Int* 114 (20) (2017) 354–361.
- [8] Y. Zhang, J.Q. Chen, J.Y. Yang, J.H. Liao, T.H. Wu, X.B. Yu, Z.W. Huang, Q. He, Q. Wang, W.J. Song, J. Luo, Q.W. Tao, Sex difference in primary Sjögren syndrome: a medical records review study, *J. Clin. Rheumatol.* 29 (5) (2023) e78–e85.
- [9] S.L. Ryan, S. Bhattacharyya, Connective tissue disorders in pregnancy, *Neurol. Clin.* 37 (1) (2019) 121–129.
- [10] J.E. Brandt, R. Priori, G. Valesini, D. Fairweather, Sex differences in Sjögren's syndrome: a comprehensive review of immune mechanisms, *Biol. Sex Differ.* 6 (2015) 19.
- [11] G.M. de Frémont, N. Costedoat-Chalumeau, E. Lazaro, R. Belkhir, G. Guettrot-Imbert, N. Morel, G. Nocturne, A. Molto, T. Goulenok, E. Diot, L. Perard, N. Ferreira-Maldent, M. Le Besnerais, N. Limal, N. Martis, N. Abisror, O. Debouverie, C. Richez, V. Sobanski, F. Maurier, G. Sauvetre, H. Levesque, M.A. Timsit, N. Tuelié, P. Orquevaux, B. Bienvenu, M. Mahevas, T. Papo, C. Lartigau-Roussin, E. Chauvet, E. Berthoux, F. Sarrot-Reynauld, L. Raffray, M. Couderc, N. M. Silva, N. Jourde-Chiche, N. Belhomme, T. Thomas, V. Poindron, V. Queyrel-Moranne, J. Delforge, C. Le Ray, E. Pannier, X. Mariette, V. Le Guern, R. Seror, Pregnancy outcomes in women with primary Sjögren's syndrome: an analysis of data from the multicentre, prospective, GR2 study, *Lancet Rheumatol* 5 (6) (2023) e330–e340.
- [12] S.S. McCoy, E. Sampene, A.N. Baer, Association of Sjögren's syndrome with reduced lifetime sex hormone exposure: a case-control study, *Arthritis Care Res.* 72 (9) (2020) 1315–1322.
- [13] S. Taiym, N. Haghighat, I. Al-Hashimi, A comparison of the hormone levels in patients with Sjögren's syndrome and healthy controls, *Oral Surg. Oral Med. Oral Pathol. Oral Radiol. Endod.* 97 (5) (2004) 579–583.
- [14] S.S. McCoy, S. Hetzel, J.J. VanWormer, C.M. Bartels, Sex hormones, body mass index, and related comorbidities associated with developing Sjögren's disease: a nested case-control study, *Clin. Rheumatol.* 41 (10) (2022) 3065–3074.
- [15] M.N. Manoussakis, M. Tsinti, E.K. Kapsogeorgou, H.M. Moutsopoulos, The salivary gland epithelial cells of patients with primary Sjögren's syndrome manifest significantly reduced responsiveness to 17 $\beta$ -estradiol, *J. Autoimmun.* 39 (1–2) (2012) 64–68.
- [16] W. Wei, T. Cao, J.L. Pathak, X. Liu, T. Mao, N. Watanabe, X. Li, M. Zhang, J. Li, Apigenin, a single active component of herbal extract, alleviates xerostomia via ER $\alpha$ -mediated upregulation of AQP5 activation, *Front. Pharmacol.* 13 (2022) 818116.
- [17] Y. Hayashi, R. Arakaki, N. Ishimaru, Apoptosis and estrogen deficiency in primary Sjögren syndrome, *Curr. Opin. Rheumatol.* 16 (5) (2004) 522–526.
- [18] S. Czerwinski, S. Mostafa, V.S. Rowan, A.M. Azzarolo, Time course of cytokine upregulation in the lacrimal gland and presence of autoantibodies in a predisposed mouse model of Sjögren's Syndrome: the influence of sex hormones and genetic background, *Exp. Eye Res.* 128 (2014) 15–22.
- [19] J.M. Kim, S.C. Shin, Y.I. Cheon, H.S. Kim, G.C. Park, H.K. Kim, J. Han, J.E. Seol, E.A. Vasileva, N.P. Mishchenko, S.A. Fedoreyev, V.A. Stonik, B.J. Lee, Effect of echinchrome A on submandibular gland dysfunction in ovariectomized rats, *Mar. Drugs* 20 (12) (2022).
- [20] S.D. Luo, T.J. Chiu, W.C. Chen, C.S. Wang, Sex differences in otolaryngology: focus on the emerging role of estrogens in inflammatory and pro-resolving responses, *Int. J. Mol. Sci.* 22 (16) (2021).
- [21] R.T. Chlebowski, G.L. Anderson, A.K. Aragaki, J.E. Manson, M.L. Stefanick, K. Pan, W. Barrington, L.H. Kuller, M.S. Simon, D. Lane, K.C. Johnson, T.E. Rohan, M.L.S. Gass, J.A. Cauley, E.D. Paskett, M. Sattari, R.L. Prentice, Association of menopausal hormone therapy with breast cancer incidence and mortality during long-term follow-up of the women's health initiative randomized clinical trials, *JAMA* 324 (4) (2020) 369–380.
- [22] J.E. Rossouw, G.L. Anderson, R.L. Prentice, A.Z. LaCroix, C. Kooperberg, M.L. Stefanick, R.D. Jackson, S.A. Beresford, B.V. Howard, K.C. Johnson, J.M. Kotchen, J. Ockene, Risks and benefits of estrogen plus progestin in healthy postmenopausal women: principal results from the Women's Health Initiative randomized controlled trial, *JAMA* 288 (3) (2002) 321–333.
- [23] Q. Zhan, J. Zhang, Y. Lin, W. Chen, X. Fan, D. Zhang, Pathogenesis and treatment of Sjögren's syndrome: review and update, *Front. Immunol.* 14 (2023) 1127417.
- [24] P. Basu, C. Maier, Phytoestrogens and breast cancer: in vitro anticancer activities of isoflavones, lignans, coumestans, stilbenes and their analogs and derivatives, *Biomed. Pharmacother.* 107 (2018) 1648–1666.
- [25] Y. Wang, X.J. Liu, J.B. Chen, J.P. Cao, X. Li, C.D. Sun, Citrus flavonoids and their antioxidant evaluation, *Crit. Rev. Food Sci. Nutr.* 62 (14) (2022) 3833–3854.
- [26] S.J. Maleki, J.F. Crespo, B. Cabanillas, Anti-inflammatory effects of flavonoids, *Food Chem.* 299 (2019) 125124.
- [27] L. Wang, J. Song, A. Liu, B. Xiao, S. Li, Z. Wen, Y. Lu, G. Du, Research progress of the antiviral bioactivities of natural flavonoids, *Nat Prod Bioprospect* 10 (5) (2020) 271–283.
- [28] N. Shen, T. Wang, Q. Gan, S. Liu, L. Wang, B. Jin, Plant flavonoids: classification, distribution, biosynthesis, and antioxidant activity, *Food Chem.* 383 (2022) 132531.
- [29] W.B. Zhuang, Y.H. Li, X.C. Shu, Y.T. Pu, X.J. Wang, T. Wang, Z. Wang, The classification, molecular structure and biological biosynthesis of flavonoids, and their roles in biotic and abiotic stresses, *Molecules* 28 (8) (2023).
- [30] D.P. Belobrajdic, A.R. Bird, The potential role of phytochemicals in wholegrain cereals for the prevention of type-2 diabetes, *Nutr. J.* 12 (2013) 62.
- [31] L. Yang, K.F. Allred, L. Dykes, C.D. Allred, J.M. Awika, Enhanced action of apigenin and naringenin combination on estrogen receptor activation in non-malignant colonocytes: implications on sorghum-derived phytoestrogens, *Food Funct.* 6 (3) (2015) 749–755.
- [32] M. Yu, H. Qi, X. Gao, Daidzein promotes milk synthesis and proliferation of mammary epithelial cells via the estrogen receptor  $\alpha$ -dependent NF $\kappa$ B1 activation, *Anim. Biotechnol.* 33 (1) (2022) 43–52.
- [33] B.S. Fegade, S.B. Jadhav, S.Y. Chaudhari, T.T. D. P. Shantaram Uttekar, S. Tabrez, M.S. Khan, S.K. Zaidi, N. Mukerjee, A. Ghosh, Synthesis and computational insights of flavone derivatives as potential estrogen receptor alpha (ER- $\alpha$ ) antagonist, *J. Biomol. Struct. Dyn.* (2023) 1–10.
- [34] Y.B. Laskar, P.B. Mazumder, A.D. Talukdar, Hibiscus sabdariffa anthocyanins are potential modulators of estrogen receptor alpha activity with favourable toxicology: a computational analysis using molecular docking, ADME/Tox prediction, 2D/3D QSAR and molecular dynamics simulation, *J. Biomol. Struct. Dyn.* 41 (2) (2023) 611–633.
- [35] J.A. Ross, C.M. Kasum, Dietary flavonoids: bioavailability, metabolic effects, and safety, *Annu. Rev. Nutr.* 22 (2002) 19–34.
- [36] D. Bafna, F. Ban, P.S. Rennie, K. Singh, A. Cherkasov, Computer-Aided ligand discovery for estrogen receptor alpha, *Int. J. Mol. Sci.* 21 (12) (2020).
- [37] A. Vidal-Limon, J.E. Aguilar-Toalá, A.M. Liceaga, Integration of molecular docking analysis and molecular dynamics simulations for studying food proteins and bioactive peptides, *J. Agric. Food Chem.* 70 (4) (2022) 934–943.
- [38] M.A. Zígolo, M.R. Goytia, H.R. Poma, V.B. Rajal, V.P. Irazusta, Virtual screening of plant-derived compounds against SARS-CoV-2 viral proteins using computational tools, *Sci. Total Environ.* 781 (2021) 146400.
- [39] S. Shakil, M.A. Kamal, S. Tabrez, A.M. Abuzenadah, A.G. Chaudhary, G.A. Damanhour, Molecular interaction of the antineoplastic drug, methotrexate with human brain acetylcholinesterase: a docking study, *CNS Neurol. Disord.: Drug Targets* 11 (2) (2012) 142–147.
- [40] T.A. Collier, T.J. Piggot, J.R. Allison, Molecular dynamics simulation of proteins, *Methods Mol. Biol.* 2073 (2020) 311–327.

- [41] A. Sali, Modeling mutations and homologous proteins, *Curr. Opin. Biotechnol.* 6 (4) (1995) 437–451.
- [42] F.I. Khan, D.Q. Wei, K.R. Gu, M.I. Hassan, S. Tabrez, Current updates on computer aided protein modeling and designing, *Int. J. Biol. Macromol.* 85 (2016) 48–62.
- [43] S. Kim, P.A. Thiessen, E.E. Bolton, J. Chen, G. Fu, A. Gindulyte, L. Han, J. He, S. He, B.A. Shoemaker, J. Wang, B. Yu, J. Zhang, S.H. Bryant, PubChem substance and compound databases, *Nucleic Acids Res.* 44 (D1) (2016) D1202–D1213.
- [44] S. Forli, R. Huey, M.E. Pique, M.F. Sanner, D.S. Goodsell, A.J. Olson, Computational protein-ligand docking and virtual drug screening with the AutoDock suite, *Nat. Protoc.* 11 (5) (2016) 905–919.
- [45] A. Waterhouse, M. Bertoni, S. Bienert, G. Studer, G. Tauriello, R. Gumienny, F.T. Heer, T.A.P. de Beer, C. Rempfer, L. Bordoli, R. Lepore, T. Schwede, SWISS-MODEL: homology modelling of protein structures and complexes, *Nucleic Acids Res.* 46 (W1) (2018) W296–w303.
- [46] S.K. Burley, H.M. Berman, G.J. Kleywegt, J.L. Markley, H. Nakamura, S. Velankar, Protein Data Bank (PDB): the single global macromolecular structure archive, *Methods Mol. Biol.* 1607 (2017) 627–641.
- [47] Y. Hu, H. Yang, X. Ding, J. Liu, X. Wang, L. Hu, M. Liu, C. Zhang, Anti-inflammatory octahydroindolizine alkaloid enantiomers from *Dendrobium crepidatum*, *Bioorg. Chem.* 100 (2020) 103809.
- [48] Y. Liu, J. Yang, M. Chen, X. Lu, Z. Wei, C. Tang, P. Yu, Recent advances in computer-aided virtual screening and docking optimization for aptamer, *Curr. Top. Med. Chem.* 23 (20) (2023) 1985–2000.
- [49] K.Y. Hsin, Y. Matsuoka, Y. Asai, K. Kamiyoshi, T. Watanabe, Y. Kawaoka, H. Kitano, systemsDock: a web server for network pharmacology-based prediction and analysis, *Nucleic Acids Res.* 44 (W1) (2016) W507–W513.
- [50] Y. Wang, Y. Wang, HBCalculator: a tool for hydrogen bond distribution calculations in molecular dynamics simulations, *J. Chem. Inf. Model.* 64 (6) (2024) 1772–1777.
- [51] S.A. Ali, M.I. Hassan, A. Islam, F. Ahmad, A review of methods available to estimate solvent-accessible surface areas of soluble proteins in the folded and unfolded states, *Curr. Protein Pept. Sci.* 15 (5) (2014) 456–476.
- [52] M. Muchtaridi, H.N. Syahidah, A. Subarnas, M. Yusuf, S.D. Bryant, T. Langer, Molecular docking and 3D-pharmacophore modeling to study the interactions of chalcone derivatives with estrogen receptor alpha, *Pharmaceuticals* 10 (4) (2017).
- [53] Q. Xue, X. Liu, P. Russell, J. Li, W. Pan, J. Fu, A. Zhang, Evaluation of the binding performance of flavonoids to estrogen receptor alpha by Autodock, Autodock Vina and Surflex-Dock, *Ecotoxicol. Environ. Saf.* 233 (2022) 113323.
- [54] N. Ishimaru, R. Arakaki, M. Watanabe, M. Kobayashi, K. Miyazaki, Y. Hayashi, Development of autoimmune exocrinopathy resembling Sjögren's syndrome in estrogen-deficient mice of healthy background, *Am. J. Pathol.* 163 (4) (2003) 1481–1490.
- [55] M. Tsinti, E. Kassi, P. Korkolopoulou, E. Kapsogeorgou, P. Moutsatsou, E. Patsouris, M.N. Manoussakis, Functional estrogen receptors alpha and beta are expressed in normal human salivary gland epithelium and apparently mediate immunomodulatory effects, *Eur. J. Oral Sci.* 117 (5) (2009) 498–505.
- [56] A.M. Brzozowski, A.C. Pike, Z. Dauter, R.E. Hubbard, T. Bonn, O. Engström, L. Ohman, G.L. Greene, J.A. Gustafsson, M. Carlquist, Molecular basis of agonism and antagonism in the oestrogen receptor, *Nature* 389 (6652) (1997) 753–758.
- [57] F. Khallouki, L. Hajji, S. Saber, T. Bouddine, M. Edderkaoui, M. Bourhia, N. Mir, A. Lim, A. El Midaoui, J.P. Giesy, M.A.M. Aboul-Soud, S. Silvente-Poirot, M. Poirot, An update on tamoxifen and the chemo-preventive potential of vitamin E in breast cancer management, *J Pers Med* 13 (5) (2023).
- [58] T. Ehtezazi, K. Rahman, R. Davies, A.G. Leach, The pathological effects of circulating hydrophobic bile acids in Alzheimer's disease, *J Alzheimers Dis Rep* 7 (1) (2023) 173–211.
- [59] P. Richardson, Applications of fluorine to the construction of bioisosteric elements for the purposes of novel drug discovery, *Expert Opin Drug Discov* 16 (11) (2021) 1261–1286.
- [60] Z. Lai, H. Yin, J. Cabrera-Pérez, M.C. Guimaro, S. Afione, D.G. Michael, P. Glenton, A. Patel, W.D. Swaim, C. Zheng, C.Q. Nguyen, F. Nyberg, J.A. Chiorini, Aquaporin gene therapy corrects Sjögren's syndrome phenotype in mice, *Proc Natl Acad Sci U S A* 113 (20) (2016) 5694–5699.
- [61] X.X. Jiang, X.W. Fei, L. Zhao, X.L. Ye, L.B. Xin, Y. Qu, K.H. Xu, R.J. Wu, J. Lin, Aquaporin 5 plays a role in estrogen-induced ectopic implantation of endometrial stromal cells in endometriosis, *PLoS One* 10 (12) (2015) e0145290.
- [62] K. Hosoi, C. Yao, T. Hasegawa, H. Yoshimura, T. Akamatsu, Dynamics of salivary gland AQP5 under normal and pathologic conditions, *Int. J. Mol. Sci.* 21 (4) (2020).